

VIBRATION REDUCTION OF A LYNX AIRCRAFT VIA ACTIVELY CONTROLLED TRAILING EDGE FLAPS

Mark P. Jones¹ and Simon J. Newman²

¹ University of Southampton,
Aerodynamics and Flight Mechanics Research Group,
University of Southampton, SO17 1BJ, United Kingdom
e-mail: M.P.Jones@soton.ac.uk

² University of Southampton,
Aerodynamics and Flight Mechanics Research Group,
University of Southampton, SO17 1BJ, United Kingdom
e-mail: S.J.Newman@soton.ac.uk

Key words: Active, Rotor, Flaps, Vibration

Abstract: The Defence Aerospace Research Partnership¹ (DARP) brings together academia and industry of the United Kingdom in a number of research areas. As part of this contract the University of Southampton is to apply models for smart rotor devices to the in-house rotor performance code of Westland Helicopters Limited (R150). One such device is the actively controlled Trailing Edge Flap (TEF) for which a variety of aerodynamics and inertia models have been incorporated into the code. The paper presents the results of an investigation, which has been conducted for evaluation of the flap models, into the use of TEFs for vibration reduction of a Lynx helicopter.

The results were found to be generally comparable to those found in the literature. In particular, the TEF is generally more effective at reducing single hub loads than multiple hub loads and the flap size was found to be of importance only when the actuator becomes saturated. At an advance ratio of 0.15 a 3/rev actuation was found to be dominant as vibration reduction was achieved through reducing the contribution of the second flapping mode to the various hub loads. At an advance ratio of 0.25 alterations to the phasing of modal contributions to the vibratory torque indicated that smaller reductions in vibration were possible when single input harmonics are used. Increases in rotor power were found to be no more than 0.5% if the flap is located in its optimum position whilst the use of dual flaps allows for greater flexibility and can operate astride the node of a dominant mode.

¹ This work was conducted under the Smart Rotor program funded by the Defence Aerospace Research Partnership DARP, contract number KK71R091

1 INTRODUCTION

The development of helicopter rotors has reached a stage where alterations to the shape and dynamic properties of the rotor blades yield steadily less significant gains in terms of overall performance. In the last decade there has been a proliferation in the literature of papers concerning a wide variety of techniques which may be said to fall under the title of ‘Smart Rotors’. With the use of these techniques large improvements are predicted in the fields of vibration reduction, noise reduction and in the overall performance of the helicopter.

Kaynes⁽¹⁾ presents a summary of the status of smart rotor research in the United Kingdom as it was in 2002. The main aspects of smart rotor technology to be explored in this reference were the use of Trailing Edge Flaps (TEFs) and Air Jet Vortex Generators (AJVGs). The Defence Aerospace Research Partnership (DARP) brings together academia and industry in a number of research areas. The role of the University of Southampton under the smart rotor theme of the DARP contract is to develop and apply models for TEFs and AJVGs to R150, the in-house rotor performance code of Westland Helicopters Limited. Use is to be made of data from other partners of the contract so that the effects on the rotor performance as a whole may be quantified.



Figure 1: A Royal Navy Lynx, photo courtesy of AgustaWestland.

An investigation into the use of a TEF for vibration reduction of a Lynx helicopter has been conducted for comparison with results found in the literature in order to evaluate the flap models incorporated into the rotor performance code. This paper will present some of the results obtained during this investigation.

2 VIBRATION REDUCTION USING SMART ROTOR TECHNIQUES

Traditional methods of reducing vibration in rotorcraft are through the use of passive vibration absorbers or isolators. Absorbers consist of masses, strategically placed, to absorb the dominant frequencies of vibration while isolators separate the fuselage from the propulsion, gearbox and rotor assembly through tuned springs or beams. Various methods of these types are described by Newman⁽²⁾. More recently, vibration reduction has been achieved through active control methods such as the Active Control of Structural Response (ACSR) system of the EH101 as described by Staple⁽³⁾.

The methods of concern here however reduce vibration at the source through control of the aerodynamic forcing and the associated blade dynamic response. A discussion of the main methods and reviews of the progress in each are given by Friedmann and Millott⁽⁴⁾. The main methods introduced are Higher Harmonic Control (HHC) from the blade root, Individual Blade Control (IBC) from the blade root, or the use of an actively controlled flap (ACF) to provide similar effects. HHC, see for example Nguyen and Chopra⁽⁵⁾, sends cyclic pitch inputs to the blades which contain components higher than 1/rev. This method is the most mature but has not been implemented due to cost and restrictions of the conventional swashplate. IBC, for example Bittanti and Cuzzola⁽⁶⁾, controls the pitch of each blade individually and has seen less emphasis due to a reluctance to replace the swashplate with electrical methods, thus causing airworthiness issues. An alternative method is to use actively controlled twist, see for example Bernhard and Wong⁽⁷⁾, which uses embedded actuators to control the twist of a blade within flight. This however imposes structural issues and requires a blade which is reasonably soft in torsion. With the use of an ACF normal control remains with the conventional swashplate and structural issues associated with an actively controlled twist rotor are reduced. It has thus become the main focus of research in this area over recent years.

3 THE ACTIVELY CONTROLLED TRAILING EDGE FLAP

In the previous decade there have been numerous experimental studies to examine the concept of the ACF. In 1995 Straub⁽⁸⁾ verified the use of trailing edge flaps for vibration reduction through wind tunnel testing. In order to yield sufficient actuation authority a selection of cams were used to investigate specific flap schedules and significant reductions in the vibratory loads were found. In 2000, Fulton and Ormiston⁽⁹⁾ used lead zirconate titanate (PZT) bimorphs for actuation of an on-blade elevon. Deflection magnitudes of 5 degrees were found to be possible at the maximum rotor speed. Frequency sweeps showed that greater response of the root flapping and torsion moments were possible at frequencies close to the natural frequencies of blade. Chopra⁽¹⁰⁾ discusses the methods available in 2000 for the actuation of flaps and blade twist and suggests that actuator dynamics should be included in analyses to provide accurate load predictions.

In 2002 Koratkar and Chopra⁽¹¹⁾ equipped a blade model with piezoelectric operated flaps which could attain flap deflection magnitudes of up to 4 degrees. Experiments using active control found that larger vibration reductions are possible for a single hub load reduction than for multiple hub loads. For the 4-bladed rotor tested, the flap actuation frequency required was found to be predominantly 3/rev with lesser contributions from 4 and 5/rev. Also of interest was the higher actuation authority near the natural frequencies of the flap and torsion modes. Leconte and des Rochettes⁽¹²⁾ review another piezoelectric device which has been tested under centrifugal and aerodynamic conditions.

In 2005 Hassan⁽¹³⁾ et al carried out 2-dimensional wind tunnel tests supported by CFD to investigate the effects of flap overhang and flap thickness-to-chord ratio on its effectiveness. The main effects of both were on the hinge moments and so both factors are important for actuation power requirements.

In terms of analytical investigations, Hassan⁽¹⁴⁾ et al considered the benefits available from both leading edge and trailing edge flaps through the modification of loads due to a Blade Vortex interaction. However this was a 2-dimensional potential flow study and the effects on rotor vibratory loads was not quantified. In 1998 Milgram and Chopra⁽¹⁵⁾ conducted a parametric study for the reduction of vibration with an integral trailing edge flap using the University of Maryland Advanced Rotor Code (UMARC). The authors concluded that the amount of vibration reduction was reasonably independent of flap length, chord, and radial position as alterations in the flap geometry was mostly offset by changes in the flap actuation schedule, although some benefit was found in keeping the flap away from the node of the second out-of-plane mode. In 2000 Myrtle and Friedmann⁽¹⁶⁾ developed an aerodynamic model which could be written in state-space form. This model was tested within a fully coupled dynamic formulation. The importance of including compressibility effects and unsteady effects were highlighted as flap deflection requirements are shown to change. It was also found that for higher blade torsional frequencies, greater flap deflections are required.

More recent studies have considered the use of multiple flaps. Viswamurthy and Ganguli⁽¹⁷⁾ considered the use of up to four flaps mounted near the blade tip. It was found that using multiple flaps reduced the deflection requirements considerably thus leading to a lower actuation power requirement. Zhang⁽¹⁸⁾ et al investigated using a hybrid active/passive design process such that the blade structural qualities allow maximum use of the actively controlled flap. Deflection requirements are found to significantly reduce, particularly if the modal frequencies are placed close to the flap actuation frequencies, while greater vibration reductions may also be available. Kim⁽¹⁹⁾ et al suggest the use of a resonance actuation system for vibration reduction. The practical implementation of the concept had been previously verified and the analytical study presented found that the use of multiple flaps and the resonance system achieved greater reductions with lower hinge moments.

In addition to reducing vibration, the effect of the flap actuation on noise has also become a consideration. In 2005 Patt⁽²⁰⁾ et al considered the prediction of noise increases due to the use of an actively controlled flap for the reduction of BVI induced vibration. Dual flaps were found to yield smaller increases in noise due to smaller deflection requirements. Following on from this, Patt⁽²¹⁾ et al used a combined cost function to reduce noise and vibration simultaneously. A dual flap system was found to be effective, however the reduction in both noise and vibration were less significant when obtained simultaneously.

4 ROTOR PERFORMANCE PROGRAM R150

There are many rotor performance programs in existence with both industry and academia developing their own in-house codes. Westland's own derivative is designated as R150. As a performance program it takes inputs of blade geometry, aerofoil data, blade modal data, flight data and limited fuselage data. From this data the program calculates the aerodynamic loading, the blade response to the loading, the resulting forces and moments within the blades and through integration is able to calculate the loads and moments translated to the hub. In this manner analyses of performance, vibration and blade loads may be undertaken.

R150 is based on a non-linear dynamic formulation, similar to that of Hodges and Dowell⁽²²⁾, which enables the use of a set of modes fully coupled in flap, lag and torsion. The version under development by the University of Southampton for the DARP research program utilises the unsteady aerodynamics model developed by Beddoes⁽²³⁾ along with Vortex Ring far-wake and interactive near-wake models.

5 INCORPORATION OF MODELS FOR A TRAILING EDGE FLAP

Three models for the aerodynamic influence of a trailing edge flap have been incorporated into R150. The first model is a simple one based on thin aerofoil theory which provides changes to the zero lift angle and the pitching moment at zero angle of attack due to a given flap deflection. The second model is based on a derivation by Theodorsen⁽²⁴⁾ and includes the unsteady effects on the pitching moment. The third and highest fidelity model to be included is that developed by Hariharan and Leishman^(25,26) at the University of Maryland. All three models have been evaluated both as stand-alone programs and within R150. It was found that the higher fidelity models are required as forcing frequencies are increased. For this reason, all results presented in this paper are for the model by Hariharan and Leishman.

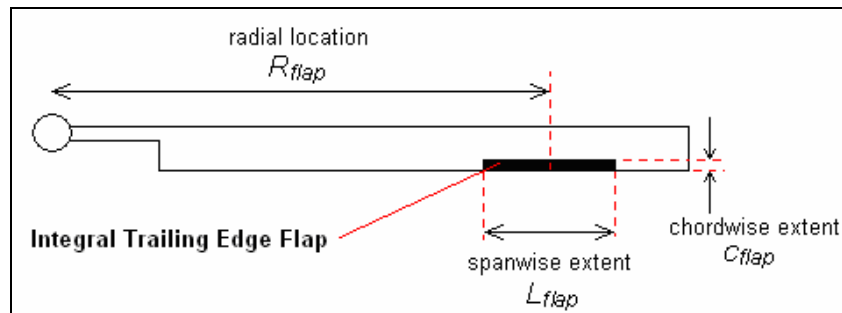


Figure 2: Geometry of a helicopter blade with integral trailing edge flap.

The chosen model gives a formulation for the changes in aerodynamic coefficients due to deflection of an integral trailing edge flap as shown in figure 2. Exact initial and asymptotic values for the changes in force and moment coefficients are known whilst assumed forms for the indicial functions approximate the temporal response. Time constants for the circulatory response are derived from experiment while those for the initial impulsive response are evaluated using linear steady subsonic theory. The model provides the necessary formulations for changes, due to flap deflection, in the normal and pressure drag forces and the pitching and flap hinge moments.

Ideally the inertia effects of a trailing edge flap would be included with an entirely new dynamic formulation which includes the properties of the trailing edge flap. This, however, is not possible under the current research program and so a simplified approach was sought. The modal properties of the blade are assumed to be unaffected by the trailing edge flap and instead any forcing due to the motion of the flap is included as a modal forcing on the right-hand-side of the equation of motion.

The derivation of the forces and moments produced by the motion of the flap mass closely follows that of Houbolt and Brooks⁽²⁷⁾, with the addition of terms for the trailing edge flap. The flap inertia forcing and the inertia contribution to the flap hinge moment are therefore functions of the flap mass, the flap centre of mass and the flap radii of gyration.

6 OPTIMISATION ALGORITHM

The optimisation algorithm being used for the scheduling of the flap deflection is based on a control method for HHC as detailed by Johnson⁽²⁸⁾. A global helicopter model is defined as equation 1, where z is a vector containing the 4/rev hub loads, z_0 is the uncontrolled response, θ is a vector containing the various harmonics of flap deflection and T is a transfer matrix.

$$z = z_0 + T\theta \quad (1)$$

A performance function may then be defined as equation 2 where W_z and W_θ are weighting matrices.

$$J = z^T W_z z + \theta^T W_\theta \theta \quad (2)$$

Substituting equation 2 into equation 1 and setting $\partial J / \partial \theta_j = 0$ for each component, j , of θ gives a set of equations which may be solved to give the optimum control vector, θ_{opt} , as shown in equation 3.

$$\theta_{opt} = -\left(T^T W_z T + W_\theta\right)^{-1} T^T W_z z_0 \quad (3)$$

Off-line identification of the transfer matrix is performed using the Least-Squares method. The transfer matrix is therefore given by equation 4, where θ_{Trial} is a matrix containing a number of trial input vectors and Z_{Trial} contains the corresponding output vectors.

$$T = Z_{Trial} \theta_{Trial} \left(\theta_{Trial}^T \theta_{Trial}\right)^{-1} \quad (4)$$

The optimisation is run outside of the performance program itself. For each trial vector an R150 run was invoked such that a valid trim case is achieved for each input. In practice 12 calculations for each input harmonic were found to be sufficient for the identification of the transfer matrix.

$$W_\theta = \begin{bmatrix} \beta & 0 \\ 0 & \beta \end{bmatrix} \quad (5)$$

The weighting matrix W_z allows the emphasis to be put onto any number of prescribed hub loads while the matrix W_θ is used to limit the flap deflection. Equation 5 shows the form of W_θ where β is calculated using the method originally suggested by Cribbs and Friedmann⁽²⁹⁾ such that $\left(\delta_{max,opt} - \delta_{max}\right)^2$ is minimised and $\delta_{max,opt}$ is the maximum scheduled flap deflection and δ_{max} is a prescribed maximum.

7 LYNX HELICOPTER TEST CASES

The data used for the investigation to be presented here correspond to that of the original metal blade of the Lynx helicopter. Four flap modes, three lag modes and one torsion mode

are included in the data, the natural frequencies for which are presented in table 1. Also to be noted are the nodal locations of the second and third flapping modes, the former being at a non-dimensional radius at around 0.825 and the latter at 0.65 and 0.875.

LAG1	FLAP1	FLAP2	LAG2	FLAP3	T1	FLAP4	LAG3
0.65	1.11	2.70	4.30	4.87	5.90	7.94	9.85

Table 1: Natural frequencies of the metal blades of the Lynx helicopter

The flight cases to be discussed are steady cruise at an altitude equivalent to 1000m ISA at advance ratios of 0.15 and 0.25. The thrust coefficient for both cases is approximately 0.0118 which corresponds to an all-up-mass of approximately 9600 lb.

The flap cases tested involve both single flaps and dual flaps. The dual flap results presented here consist only of those located directly adjacent to one another such that they are essentially a single flap split half way along its length such that either half may be individually scheduled. Note that the quoted spanwise extents for the dual flap correspond to the total length of the two flaps, as shown in figure 3.

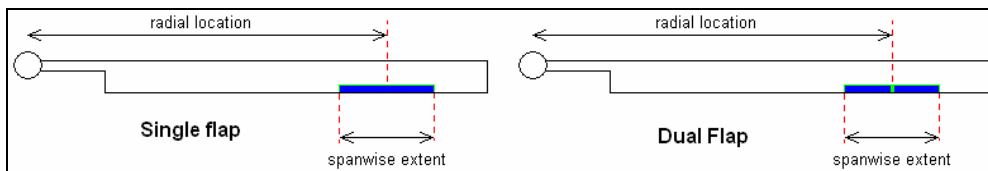


Figure 3: Geometries of the single and dual flap test cases.

All cases used a flap of chord 0.2 times the blade chord with a large flap mass per unit length of 0.2 times the blade mass per unit length as these results were used to accentuate the flap inertia effects. The maximum allowable flap deflection in all cases was set to 4 degrees. The flaps were at first actuated at individual harmonics of 2, 3, 4 and 5/rev following which operation at all four harmonics simultaneously was investigated. Flap locations varied from 0.4R to 0.9R in 0.1R steps with flap lengths of 0.1R, 0.15R and 0.2R.

8 RESULTS - ADVANCE RATIO 0.15 (64 KTS)

8.1 Blanket Results

To investigate the behaviour of the model some blanket tests were conducted for a single flap operating at a single frequency. The test matrix used was very coarse testing every 40 degrees of deflection phase and every 1 degree of deflection magnitude up to a maximum of 4 degrees. An example of the contour plots obtained is shown in figure 4 for a flap of length 0.1R located at 0.6R and operating at 3/rev. The contours show the reduction in the 4/rev component of each hub load expressed as a percentage of the value with no flap actuation. The plots display a reasonably linear behaviour over the range tested suggesting that application of the linearised optimisation algorithm is indeed applicable.

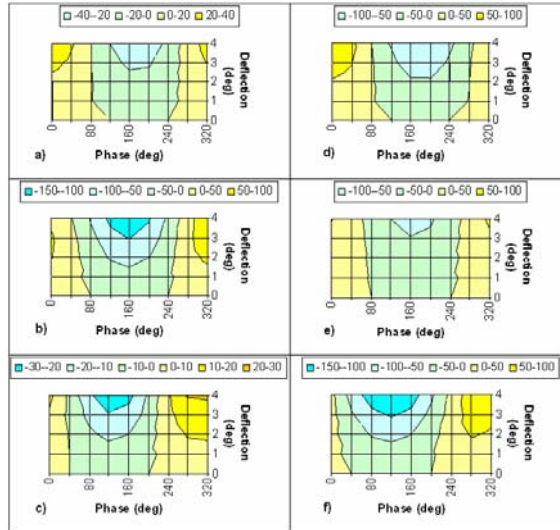


Figure 4: Blanket search results for a 20% chord flap at $x=0.6R$ and length $0.1R$ Operating at 3/rev showing reduction in fixed 4/rev hub loads. a) longitudinal shear b) lateral shear c) thrust d) rolling moment e) pitching moment f) torque. $\mu=0.15$.

Similar results were obtained at a variety of radial locations for actuation frequencies of 2, 3, 4 and 5/rev, which on collecting the maximum available reduction from each test results in the plots of figure 5. The plots on the left show the reduction available from each hub load if they are optimised individually without regard to the other hub loads. Significant reductions are available from each frequency and the significance of the node of the second flapping mode near the $0.8R$ location is immediately clear since the reduction in vibration is frequently decreased when the flap is at this radial position.

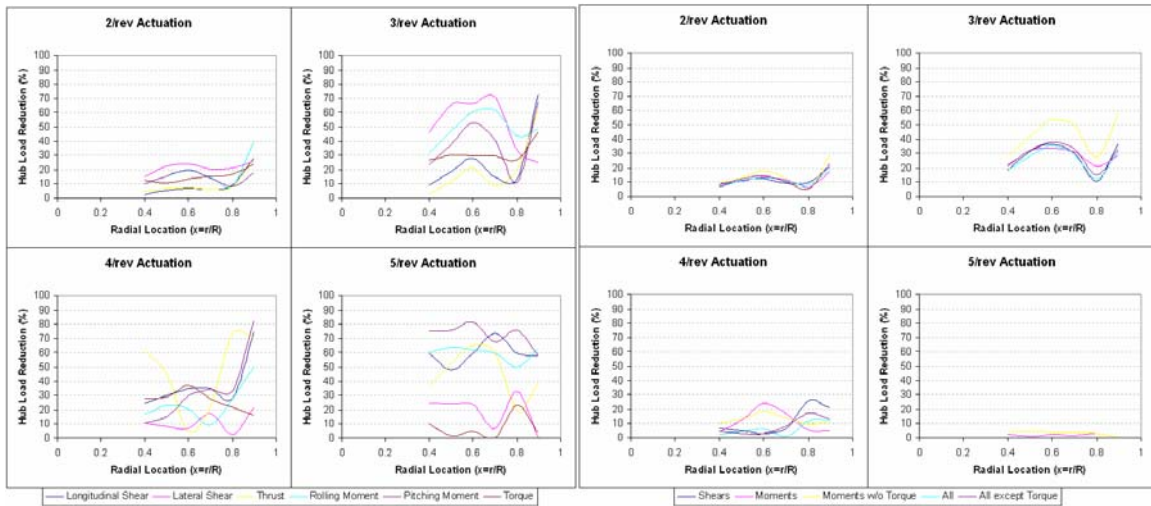


Figure 5: Blanket search results for a 20% chord, 10% radius flap showing optimum reduction of individual and combinations of fixed 4/rev hub loads, $\mu = 0.15$.

Averaging the reductions available from each hub load at each flap actuation magnitude and phase allows the optimisation for various combinations of hub loads as shown on the right-hand-side of figure 4. Firstly all three shears are reduced, then all three moments followed by just the rolling and pitching moments. The fourth optimisation reduces all six hub loads and finally all loads excluding the torque are reduced. The ability of a 3/rev actuation to reduce hub loads simultaneously is clear as is the influence of the node of the second flapping mode.

A contribution from the 2/rev actuation could be significant while the 5/rev actuation yields very little reduction.

8.2 Single Harmonic Actuation

Applying the algorithm to the optimisation of the flap deflection for various flap lengths and locations results in figure 6 for the vibration reduction. Notice that the plots, showing the optimum reduction of all six hub loads, agree reasonably well with the results from the blanket search in figure 5 for a flap of length 0.1R.

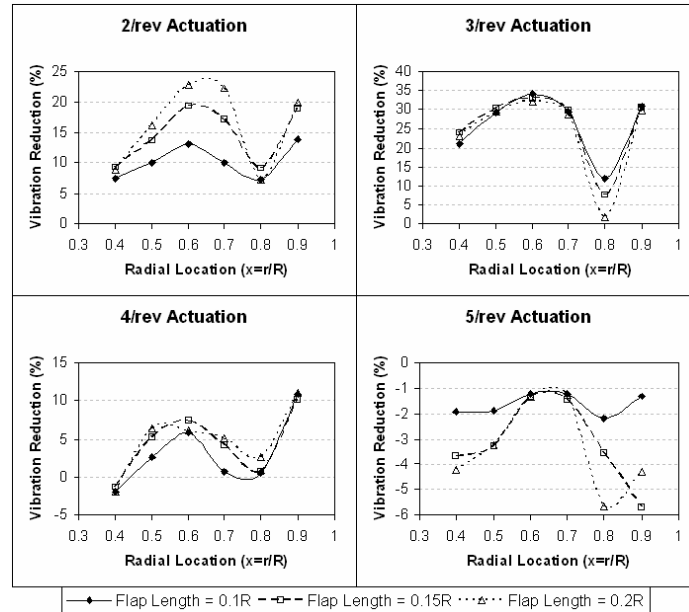


Figure 6: Optimal reduction of all six hub loads as given by the algorithm. $\mu=0.15$.

Actuation at 2, 3 and 4/rev yields reasonable reduction at locations away from the node of the second flap mode. No vibration reduction is available from a 5/rev actuation but the algorithm predicted an optimum control vector which was non-zero and resulted in slight increases in vibration.

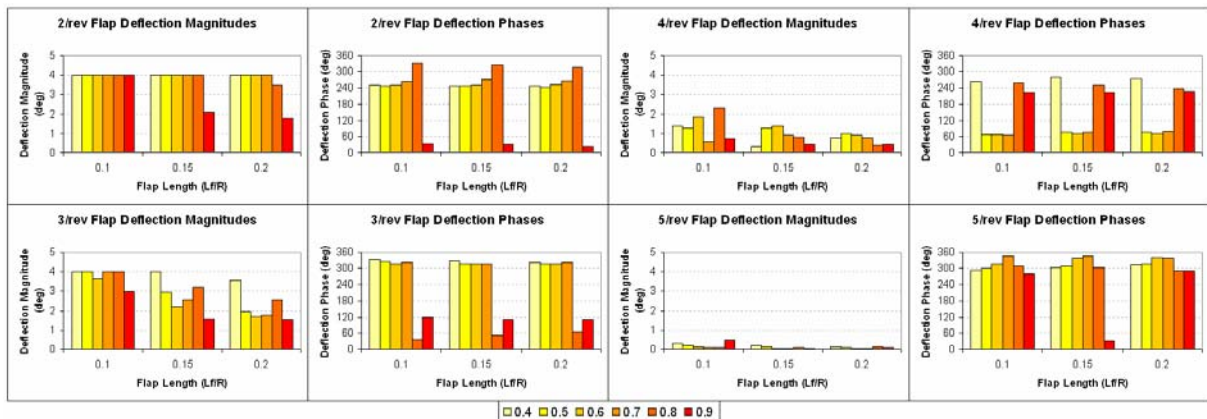


Figure 7: Optimal flap deflection magnitudes and phases for reduction of all six hub loads with various flap lengths and locations. $\mu=0.15$.

The smaller flap yielded less error in this respect, possibly due to the decreased amount of non-linearity associated with a smaller flap. For actuation frequencies of 2 and 4/rev, in-

increases in flap length led to an increase in the vibration reduction, particularly in the 2/rev case. Larger flaps gave no improvement for the 3/rev actuation however.

Figure 7 presents the actuation magnitudes and phases predicted by the algorithm. For the 2/rev case, the maximum 4 degrees of deflection is required of all flap lengths and so the larger flap is compensating for the limitation in the flap deflection to give a larger reduction in vibration. For the 3/rev case, the 4/rev maximum is reached only for the smallest flap. This means that increases in flap size are offset by smaller flap deflections such that the optimum vibration reduction is obtained for each case.

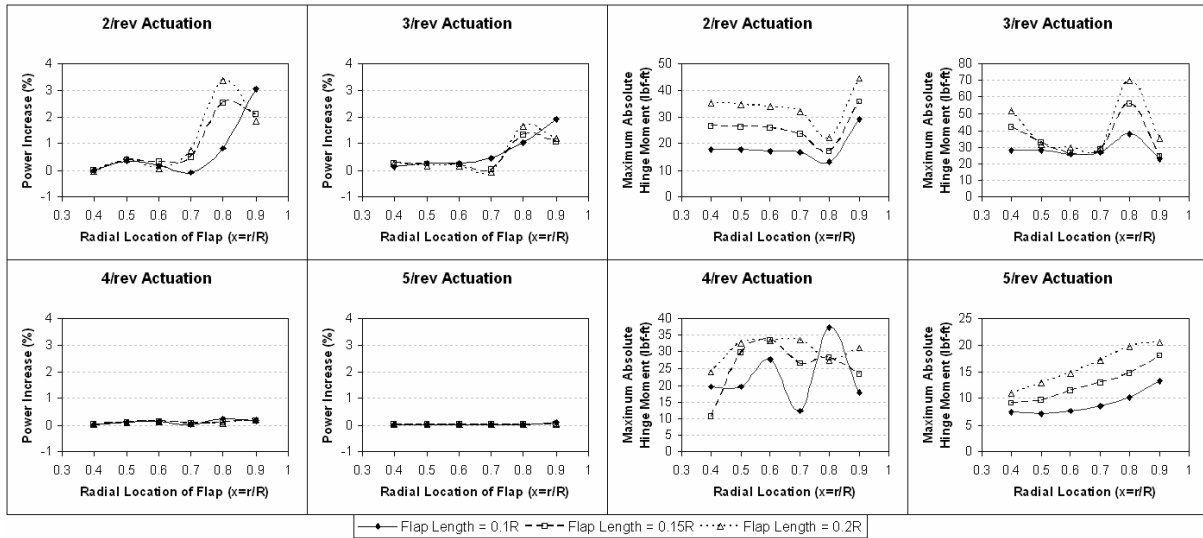


Figure 8: Rotor Power Increase and maximum absolute hinge moment due to optimal reduction of all six hub loads. $\mu=0.15$.

The use of a trailing edge flap for vibration reduction clearly has effects on other aspects of the rotor performance. Figure 8 displays the increase in rotor power for each optimised flap case. The rotor power is increased for all vibration reduction cases; however power increases greater than 1% of the total rotor power are only encountered when large flap deflection magnitudes are used at outboard locations. The optimum vibration reduction is generally encountered with the flap at the 0.6R location. At this position the rotor power increase never exceeds 0.5%.

The maximum absolute flap hinge moment is also presented in figure 8. Generally, the hinge moment for a given flap deflection would be expected to increase as the flap is increased in size and moved outboard, as increases in dynamic head and blade accelerations lead to greater aerodynamic and inertial contributions. This is reflected in the case of the 5/rev actuation as very small flap actuation angles are employed. For other flap schedules however, the phase and magnitude of the flap deflection will have a large influence and the azimuth position corresponding to the maximum hinge moment is likely to change. The maximum hinge moment is therefore a complicated function of the flap deflection schedule and its interaction with the aerodynamics and blade dynamics. There does however appear to be benefits in locating the flap near the 0.6R optimum location.

8.3 Multiple Harmonics and Multiple Flaps

Consider now a flap operating with deflection components of 2, 3, 4 and 5/rev with the maximum allowable flap deflection remaining at 4 degrees. Flap sizes of 0.1R, 0.15R and

0.2R are again investigated along with radial locations varying from 0.4R to 0.9R at 0.1R intervals. Figure 9 presents the vibration reduction, power increase, effects on the pitch link loads, optimum flap deflection angles and the resulting maximum absolute hinge moments.

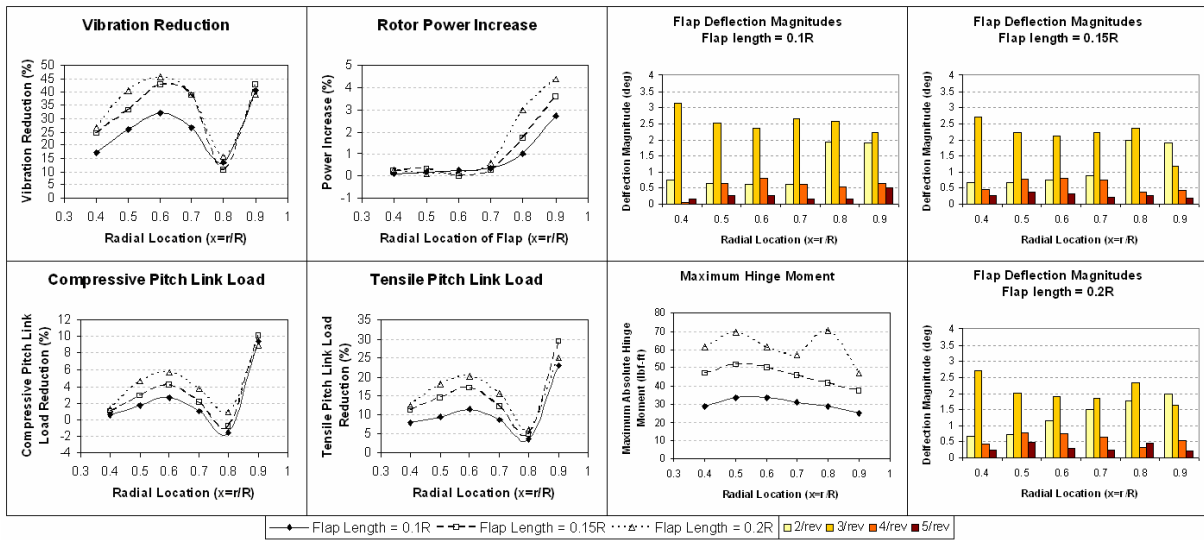


Figure 9: Effects due to optimum vibration reduction using a flap actuation at 2, 3, 4 and 5/rev simultaneously. $\mu=0.15$.

For the smallest flap, the vibration reduction when the flap is located inboard is of similar magnitude to the single 3/rev actuation. Recall that the 3/rev actuation required the entire 4 degree deflection in order to achieve the maximum vibration reduction. As the flap is increased in size however, the 3/rev frequency requires a smaller flap deflection magnitude and so components of the other frequencies may be included to yield further reductions in vibration through other means. Once again the increase in total rotor power is only significant at outboard stations and the pitch link loads mostly show reductions in both the compressive and tensile loads. From the shape of the plots the pitch link loads would appear to be directly related to the vibration reduction which is to be expected as the blade torque will contribute to the hub moments.

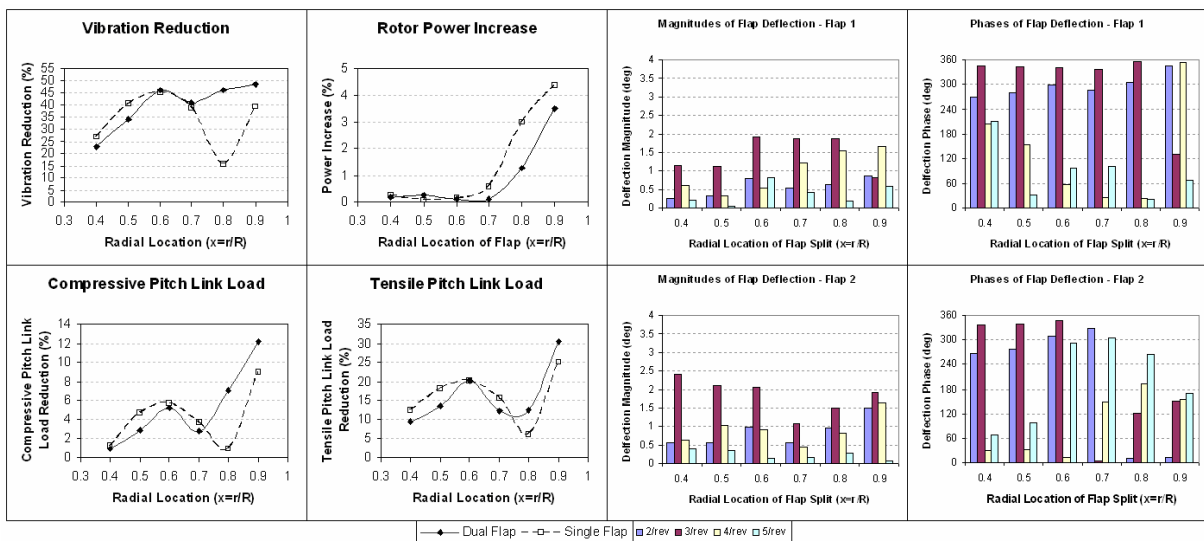


Figure 10: Effects due to optimum vibration reduction using dual flaps with actuation at 2, 3, 4 and 5/rev simultaneously. $\mu=0.15$.

Figure 10 displays the results obtained using a dual flap in comparison to a single flap of the same total length (0.2R). The performance of the dual flap is generally similar to the single flap except near the node where it is vastly superior. Note that the phase of the outboard flap is markedly different from that of the inboard flap. It is this ability which enables the dual flap to work well near the node. Figure 11 shows the maximum hinge moment of each flap. By splitting the flap the maximum hinge moments for each flap are much reduced and therefore with a given actuator the maximum flap deflections may be increased and possibly further reductions obtained.

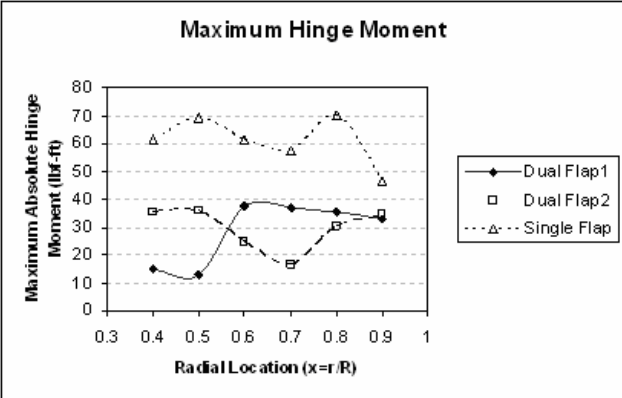


Figure 11: Maximum hinge moments using dual flaps operating at 2, 3, 4 and 5/rev simultaneously. $\mu=0.15$.

9 RESULTS - ADVANCE RATIO 0.25 (107 KTS)

9.1 Blanket Results

The contour plots for a flap of length $0.1R$ located at $0.6R$ and operating at $3/\text{rev}$ are shown in figure 12. The plots appear to be reasonably linear but are not as ordered as those for the lower advance ratio. It would appear from these plots however that the algorithm should still give reasonable results.

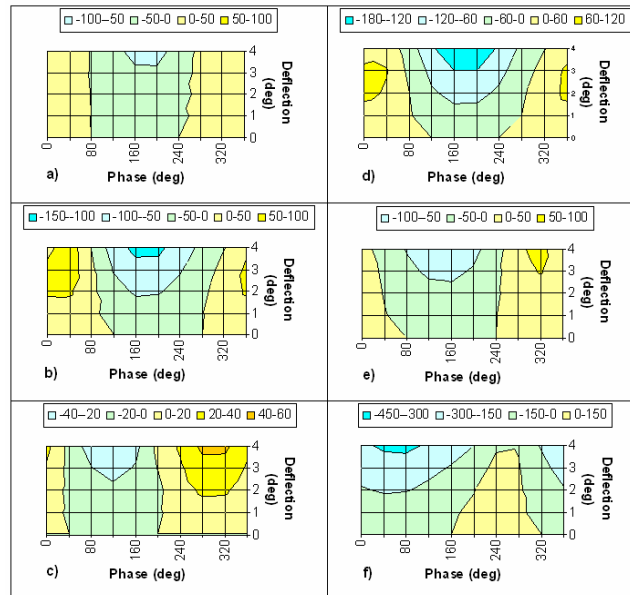


Figure 12: Blanket search results for a 20% chord flap at $x=0.6R$ and length $0.1R$ Operating at $3/\text{rev}$ showing reduction in fixed $4/\text{rev}$ hub loads. a) longitudinal shear b) lateral shear c) thrust d) rolling moment e) pitching moment f) torque. $\mu=0.25$.

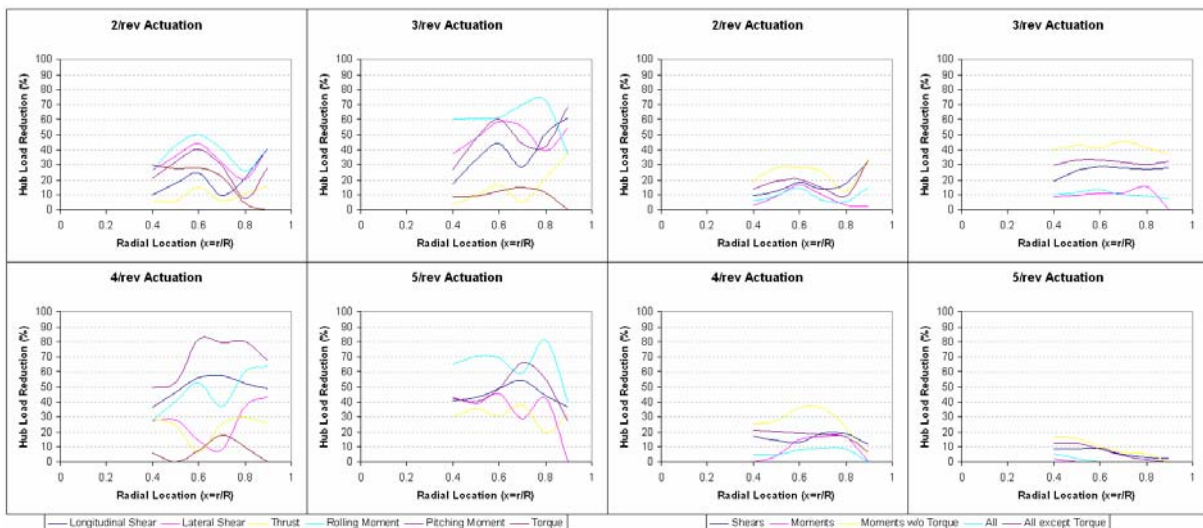


Figure 13: Blanket search results for a 20% chord, 10% radius flap showing optimum reduction of individual and combinations of fixed $4/\text{rev}$ hub loads, $\mu = 0.25$.

Collecting the blanket results for various flap locations and frequencies results in figure 13. Significant reductions are available from each frequency for individually optimised hub loads,

although the reductions in the vibratory thrust and torque are generally less than in the other loads, with the 5/rev actuation being totally incapable of reducing the vibratory torque. Optimising for combinations of hub loads again leads to much smaller reductions. The 5/rev actuation is once again mostly incapable of reducing more than one hub load simultaneously. The performance of the other frequencies in reducing the hub shears is reasonable, however all frequencies struggle to reduce all three hub moments simultaneously. If the vibratory torque is left out of the optimisation schedule however the reduction is much improved.

9.2 Single Harmonic Actuation

Using the algorithm to optimise for the reduction of all six hub loads yields the vibration reduction results presented in figure 14 and the flap deflection schedules presented in figure 15. The results obtained using the algorithm differ a fair amount from the results using the blanket search. This is most likely due to measurement errors of the program, particularly as the control angles are smaller at the higher advance ratio.

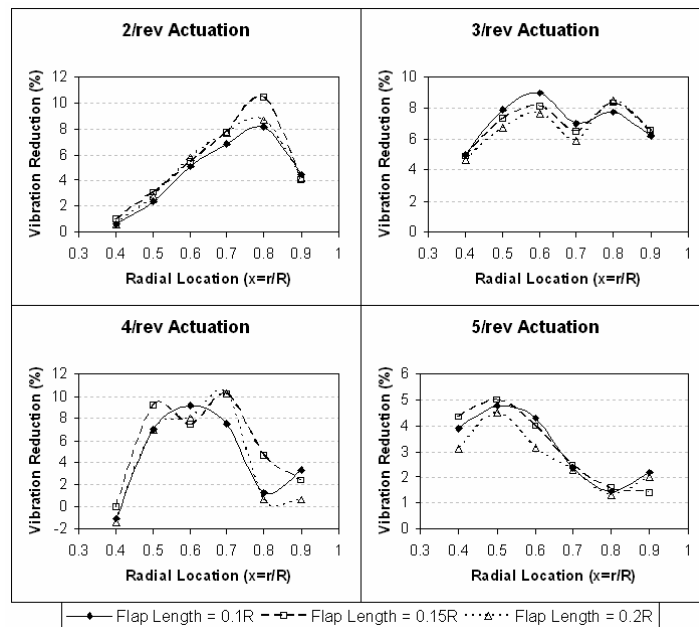


Figure 14: Optimal reduction of all six hub loads as given by the algorithm. $\mu=0.25$.

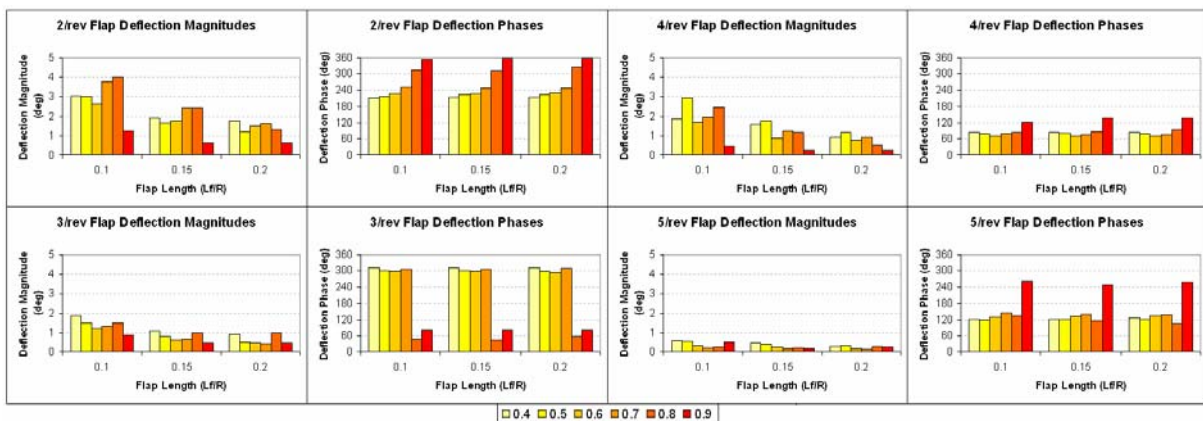


Figure 15: Optimal flap deflection magnitudes and phases for reduction of all six hub loads with various flap lengths and locations. $\mu=0.25$.

Small reductions in vibration are obtained for all frequencies at all radial locations except the innermost one at 4/rev. The magnitude of the reduction is small however and none of the actuation frequencies appear to excel at reducing all the hub loads simultaneously. The node of the second flapping mode appears to have little influence apart from at 5/rev. This would suggest that the flap is affecting different or multiple modes to produce the small amount of vibration reduction in evidence. However, the phasing of the optimum 3/rev actuation suggests that the node of the second flapping mode is important as the optimum phase changes for flaps located at the 0.8R and 0.9R radial locations. The effects on vibration reduction due to increases in flap length appear to be small and varied and show little sign of increasing the effectiveness of the flap. Figure 15 however does reveal that the increase in flap size is being compensated for by a decrease in the flap deflection.

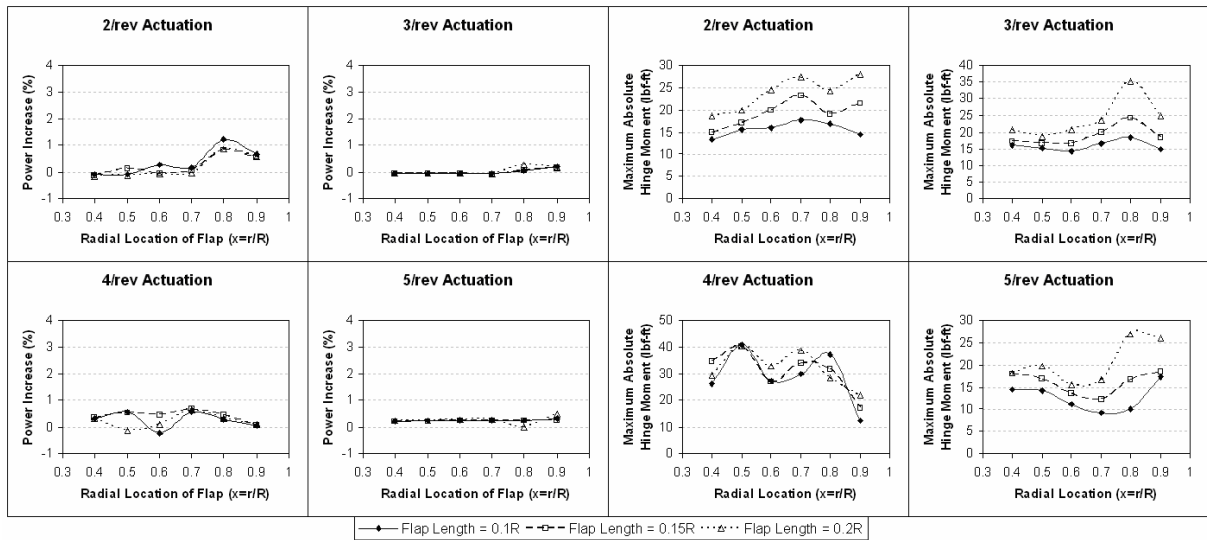


Figure 16: Rotor Power Increase and maximum absolute hinge moment due to optimal reduction of all six hub loads. $\mu=0.25$.

From figure 16 the increase in rotor power due to the actuation of the flap is small and in a few cases the power is marginally decreased. The smaller influence on the rotor power at this advance ratio is most likely due to the smaller flap deflections employed, particularly for out-board locations. The behaviour of the hinge moments is again complicated by the flap scheduling and the traces do appear to reflect the flap deflection magnitude, particularly for the 4/rev case.

9.3 Multiple Harmonics and Multiple Flaps

Results for a single flap operating at the four harmonics simultaneously are presented in figure 17. Firstly it should be noted that the algorithm appears to be incapable of predicting the optimum schedule for larger flaps at the outermost location. Elsewhere, the reduction of vibration appears to be reasonable, especially considering how actuation at the various harmonics individually yielded little advantage. The small deflection requirements of each harmonic, except 2/rev, has enabled the flap to harness the advantages of all four harmonics simultaneously for all sizes of flap. The use of larger flaps generally only gives increases in the amount of vibration reduction at the two inner stations (although the largest flap does perform well at the 0.8R location). The flap deflection schedule does not appear to be vastly reduced in amplitude for the larger flaps however. Also noteworthy is that increases in total rotor power are

only substantial at outboard stations and the changes in the pitch link loads are mostly advantageous.

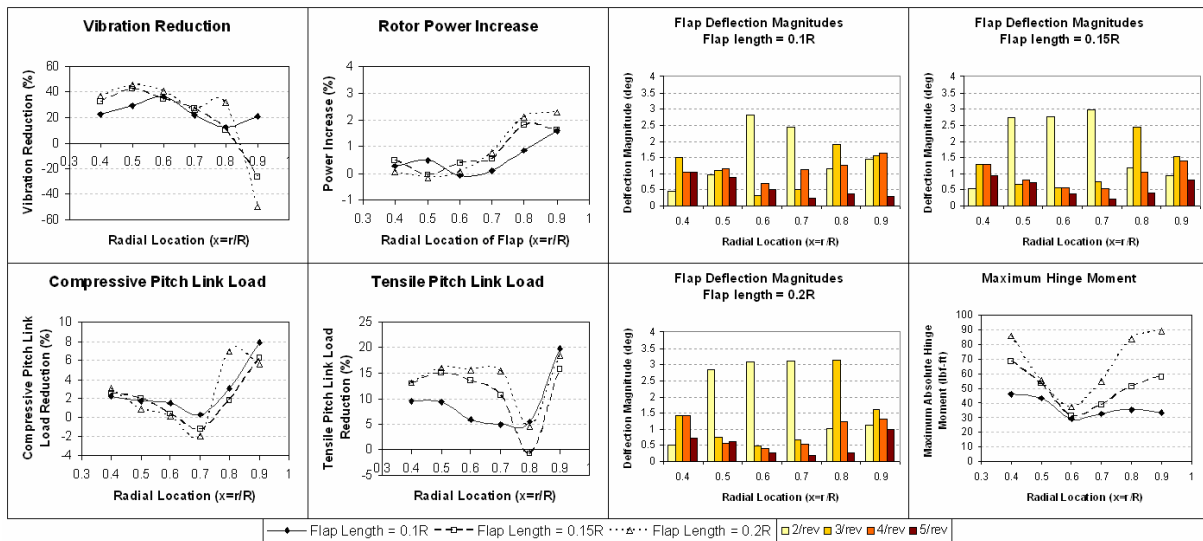


Figure 17: Effects due to optimum vibration reduction using a flap actuation at 2, 3, 4 and 5/rev simultaneously. $\mu=0.25$.

Figure 18 displays the results obtained using the dual flap in comparison to the single flap. Once again the advantages of the dual flap near the presence of a node are clear as vibration reduction is increased while the increase in rotor power is less. The reductions in the hinge moments, shown in figure 19, are not observed at all radial locations in this case, possibly due to the larger amount of higher frequency (5/rev) flap deflection.

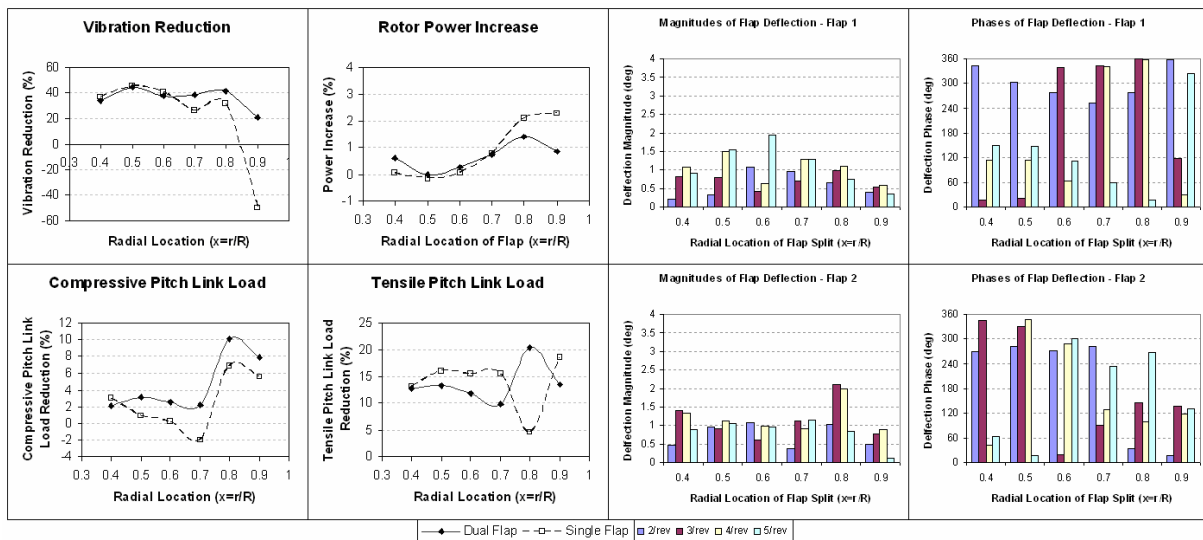


Figure 18: Effects due to optimum vibration reduction using dual flaps with actuation at 2, 3, 4 and 5/rev simultaneously. $\mu=0.25$.

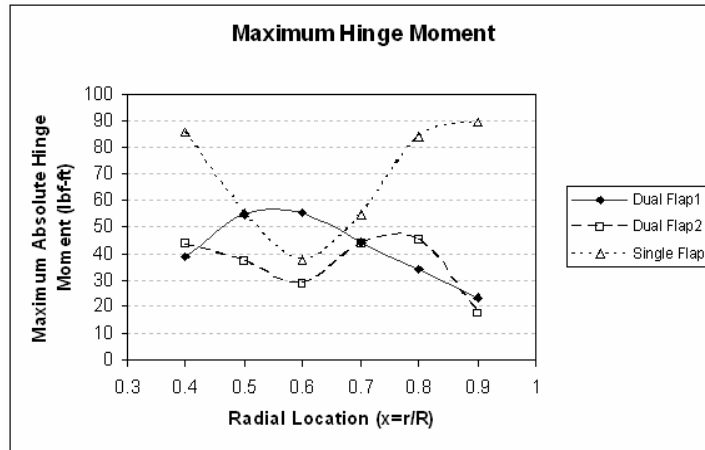


Figure 19: Maximum hinge moments using dual flaps operating at 2, 3, 4 and 5/rev simultaneously. $\mu=0.25$.

10 MODAL ANALYSIS OF CASES

The modal contributions to each hub load are presented in figures 19-22 which are plotted in polar form. These figures present the 4/rev hub responses with the sine component on the vertical axis plotted against the cosine component on the horizontal axis. The magnitude of the response is therefore the distance from the origin to the end of the trace. The magnitude due to each mode is the length of that segment and the phase is given by the direction of the segment. In this form it is easy to see the contributions of each mode and also any cancellation of the modal contributions.

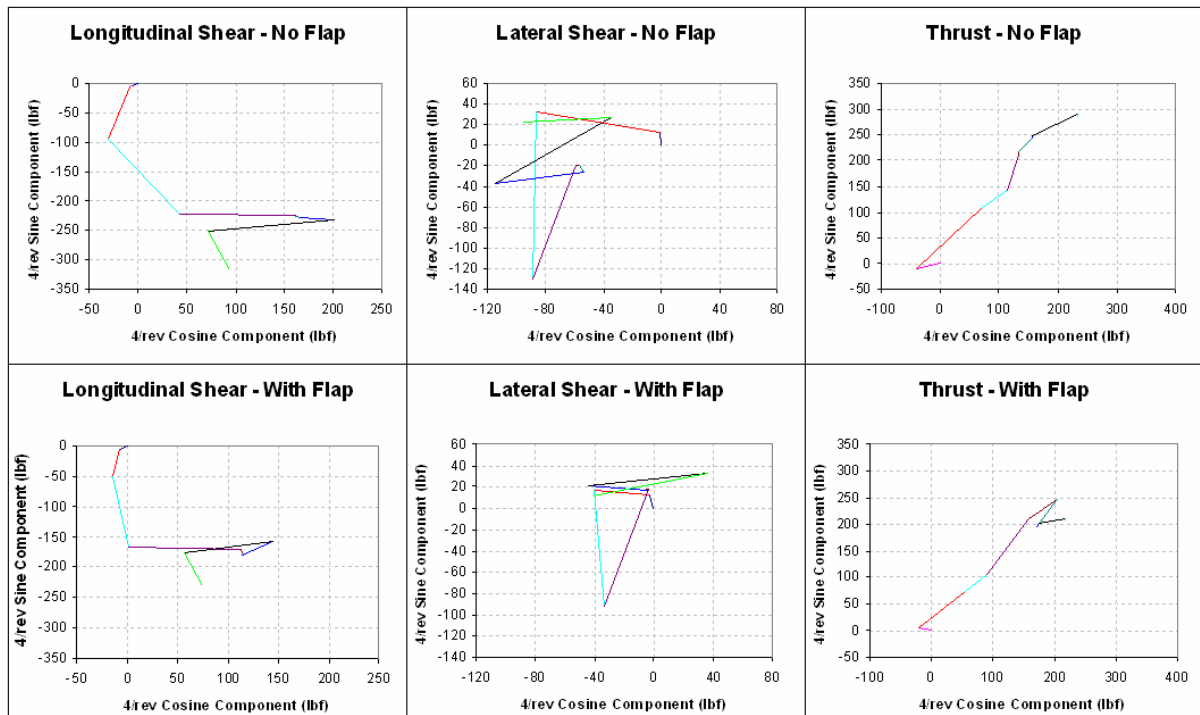


Figure 19: Modal contributions to hub shears at $\mu=0.15$.

Charts for the hub shears at an advance ratio of 0.15 are presented in figure 19. The reduction of the longitudinal shear magnitude is the result of reductions in most of the modal contributions plus a phase change in the 2nd lag mode. The lateral shear is reduced through reduc-

tions in the 2nd flapping and lagging modes together with a phase change in the higher modes. Reduction in the vibratory thrust is achieved through reductions in the second flapping and higher modes along with a phase change of the 3rd lagging mode.

Charts for the hub moments at this advance ratio are presented in figure 20. The minimum rolling and pitching moments are achieved through reductions in the 2nd flapping mode and the higher modes. The vibratory torque is partly reduced through reductions in the 2nd lag mode and the higher modes, but is mostly achieved through a phase change in the higher modes. Overall, reductions in the in-plane shears and the rolling and pitching moments are mostly achieved through the reduction of various modal contributions to the total hub loads whilst the thrust and torque are mostly reduced through the alteration of modal phasing.

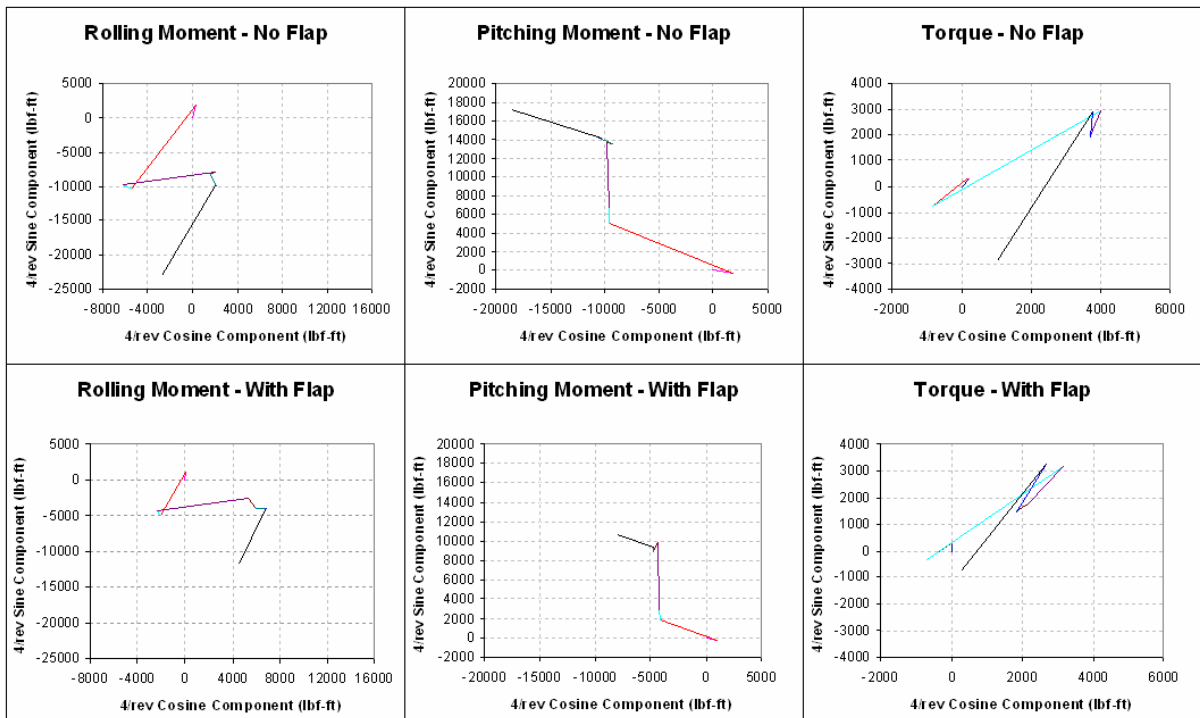


Figure 20: Modal contributions to hub moments at $\mu=0.15$.

The modal contributions to the hub shears at an advance ratio of 0.25 are presented in figure 21. Minimisation of the longitudinal shear is achieved through reductions in the 2nd flapping mode and the higher modes as well as a phase change accompanied by a slight increase in the 2nd lag mode contribution. A small improvement to the lateral shear is made through reductions in the 2nd flapping and lagging modes while there is little difference in the magnitude of the 4/rev thrust load, although there is a small phase change.

There is little reduction in the vibratory rolling moment, shown in figure 22. The vibratory pitching moment is decreased through reductions in the contributions from the 2nd flapping mode and the higher modes. The magnitude of the vibratory torque without actuation of the flap is small due to effective cancellation of the modal contributions. With the actuation of the flap, a greater reduction in the contribution of the 2nd lagging mode than that of the higher modes has caused the vibratory torque to increase. Indeed analysis of the modal contributions when using flaps actuated at individual harmonics has shown that only a 4/rev actuation can have any beneficial effects on the vibratory torque whilst reducing all six hub loads.

At the higher advance ratio, reductions in the in-plane shears and the rolling and pitching moments are again achieved using reductions in various modal contributions. However, the actuation of the flap affects the phasing of the vibratory thrust and torque modal contributions. In terms of the thrust this has little influence, however as the vibratory torque is initially small due to modal cancellation, changes in the phase are most likely to result in increases in the vibratory torque. It is therefore for this reason that lower reductions in the vibration may be achieved at this advance ratio when the vibratory torque is included in the optimisation.

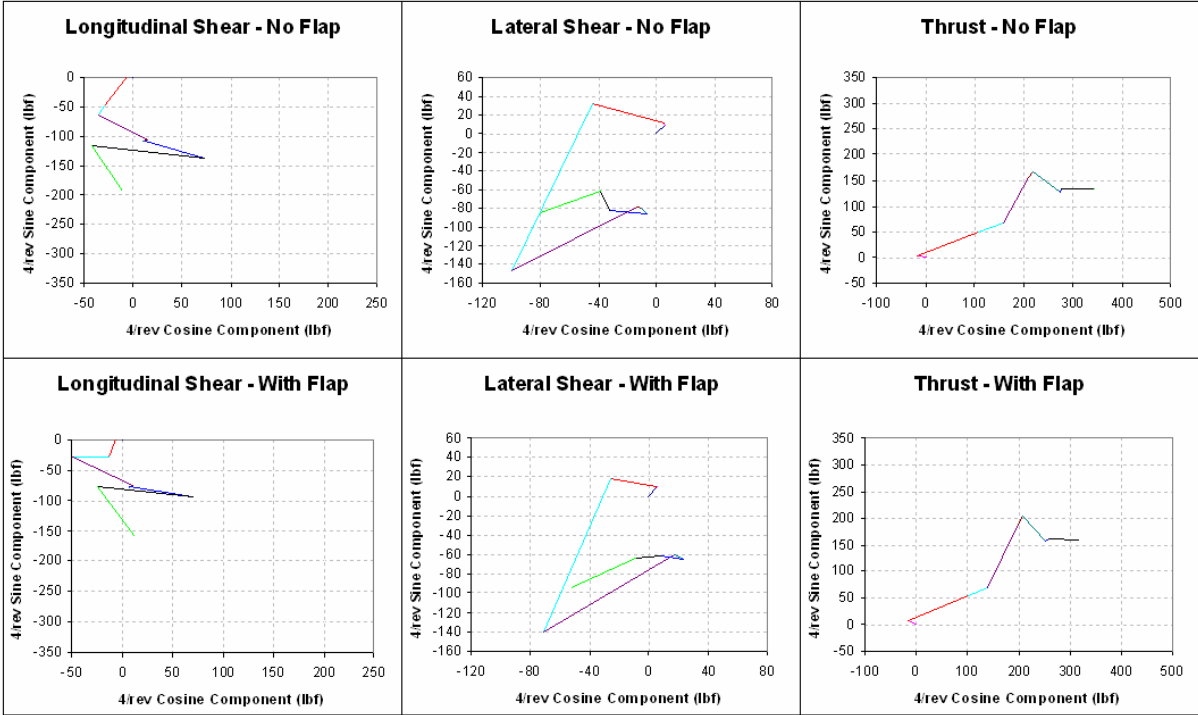


Figure 21: Modal contributions to hub shears at $\mu=0.25$.

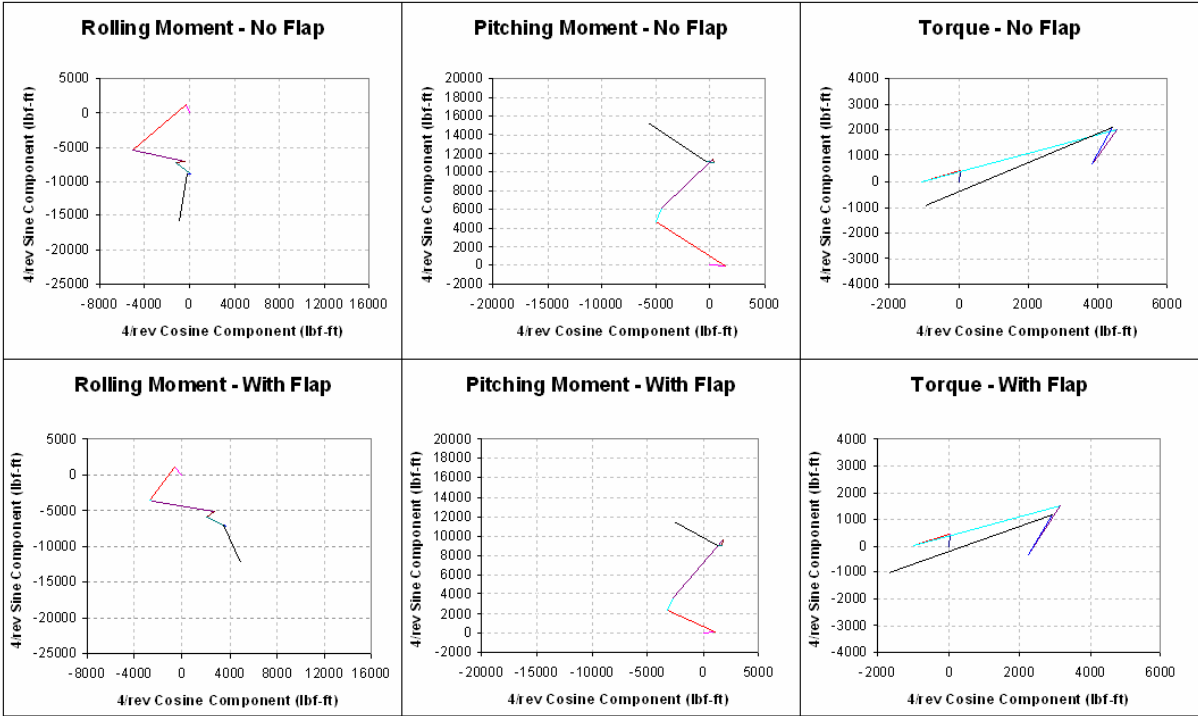


Figure 22: Modal contributions to hub moments at $\mu=0.25$.

11 CONCLUSIONS

Models for a trailing edge flap have been incorporated into R150, the rotor performance code of Westland Helicopters Limited. An investigation into vibration reduction of the Lynx helicopter using actively controlled trailing edge flaps has been conducted as part of the evaluation of the trailing edge flap models. Results were found to be generally comparable to those in the literature. In particular the following may be concluded.

- The trailing edge flap is generally more effective at reducing single hub load components than it is at reducing multiple hub load components simultaneously.
- Flap size was found to be of importance only when the actuator becomes saturated, as increases in flap size are offset with smaller flap deflections.
- The use of the trailing edge flap for vibration reduction was generally more effective at the lower advance ratio of 0.15 than for an advance ratio of 0.25.
- At the lower advance ratio, vibration reduction is achieved through the minimisation of the contribution of various modes to the 4/rev components of the in-plane shears and the rolling and pitching moments. Phase changes in the modal contributions to the vibratory thrust and torque occur as secondary effects and are generally advantageous. A 3/rev component of actuation dominates as most reduction is due to the second flapping mode which has a natural frequency closest to 3/rev. The vibration reduction is therefore much reduced if the flap is located astride the node of this mode.
- At the higher advance ratio the phase changes in the modal contributions to the vibratory torque cause significant increases such that the optimiser suggests small flap deflections which result in little vibration reduction if a single input harmonic is used. When multiple harmonics are used the vibration reduction is greater as the phasing of the torque contributions can be more controlled.
- The rotor power increase due to flap actuation is never greater than 5% if the flap is located in its optimum location at around 0.6R.
- The use of dual flaps allows for flexibility between flight conditions and can operate astride the node of a dominant mode whilst their small size leads to decreases in hinge moments.

12 REFERENCES

- [1] I. Kaynes, "Smart Rotor Research in the UK", Proceedings of the American Helicopter Society 58th Annual Forum, 2002.
- [2] S.J. Newman, "The Foundations of Helicopter Flight, Arnold, 1994.
- [3] A.E. Staple, "Evaluation of Active Control of Structural Response as a means of Reducing Helicopter Vibration", Proceedings of the American Helicopter Society 46th Annual Forum, 1990.
- [4] P.P. Friedmann and T.A. Millott, "Vibration Reduction in Rotorcraft Using Active Control: A comparison of Various Approaches", Journal of Guidance, Control and Dynamics, Volume 18, No. 4, 1995.
- [5] K. Nguyen and I. Chopra, "Application of Higher Harmonic Control to Rotors Operating at High Speed and Thrust", Journal of the American Helicopter Society, Volume 35, No. 3, 1990.
- [6] S. Bittanti, F.A. Cuzzola, "Generalised Active Control of Vibration in Helicopters", Journal of Guidance, Control and Dynamics. Volume 25, No. 2, 2002.
- [7] A. Bernhard, J. Wong, "Wind Tunnel Evaluation of a Sikorsky Active Rotor Controller

- Implemented on the NASA/ARMY/MIT Active Twist Rotor, *Journal of the American Helicopter Society*, Volume 50, No. 1, 2005.
- [8] F.K. Straub, "Active Flap Control for Vibration Reduction and Performance Improvement", *Proceedings of the American Helicopter Society 51st Annual Forum*, 1995.
- [9] M.V. Fulton, Ormiston. R.A., "Hover Testing of a Small-Scale Rotor with On-Blade Elevons", *Journal of the American Helicopter Society*, Volume 46, No. 2, 2001.
- [10] I. Chopra, "Status of Application of Smart Structures Technology to Rotorcraft Systems", *Journal of the American Helicopter Society*, Volume 45, No. 4, 2000.
- [11] N. Koratkar, I. Chopra, "Wind Tunnel Testing of a Smart Rotor Model with Trailing Edge Flaps", *Journal of the American Helicopter Society*, Volume 47, No. 4, 2002.
- [12] P. Leconte, H.M. des Rochettes, "Experimental Assessment of an Active Flap Device", *Proceedings of the American Helicopter Society 58th Annual Forum*, 2002.
- [13] A. Hassan, F. Straub and K. Noonan, "Experimental/Numerical Evaluation of Integral Trailing Edge Flaps for Helicopter Rotor Application", *Journal of the American Helicopter Society*, Volume 50, No. 1, 2005.
- [14] A. Hassan, L. Sankar and H. Tadghighi, "Effects of Leading and Trailing Edge Flaps on the Aerodynamics of Airfoil/Vortex Interactions", *Journal of the American Helicopter Society*, Volume 39, No. 2, 1994.
- [15] J. Milgram and I. Chopra, "A Parametric Design Study for Actively Controlled Trailing Edge Flaps", *Journal of the American Helicopter Society*, Volume 43, No. 2, 1998.
- [16] T. F. Myrtle and P.P. Friedmann, "Application of a New Compressible Time Domain Aerodynamic Model to Vibration Reduction in Helicopters Using an Actively Controlled Flap", *Journal of the American Helicopter Society*, Volume 46, No. 1, 2001.
- [17] S.R. Viswamurthy and R. Ganguli, "An Optimisation Approach to Vibration Reduction in Helicopter Rotors with Multiple Active Trailing Edge Flaps", *Aerospace Science and Technology*, Volume 8, 2004.
- [18] J. Zhang, E.C. Smith and K.W. Wang, "Active-Passive Hybrid Optimisation of Rotor Blades with Trailing Edge Flaps", *Journal of the American Helicopter Society*, Volume 49, No. 1, 2004.
- [19] J.S. Kim, E. Smith and K. Wang, "Helicopter Vibration Suppression via Multiple Trailing Edge Flaps Controlled by a Resonance Actuation System", *Proceedings of the American Helicopter Society 60th Annual Forum*, 2004.
- [20] D. Patt, L. Liu and P. Friedmann, "Rotorcraft Vibration Reduction and Noise Prediction Using a Unified Aeroelastic Response Simulation", *Journal of the American Helicopter Society*, Volume 50, No. 1, 2005.
- [21] D. Patt, L. Liu and P.P. Friedmann, "Simultaneous Vibration and Noise Reduction in Rotorcraft Using Aeroelastic Simulation", *Journal of the American Helicopter Society*, Volume 51, No. 2, 2006.
- [22] D.H. Hodges and E.H. Dowell, "Non-Linear Equations of Motion for the Elastic Bending and Torsion of Twisted Non-Uniform Rotor Blades", *NASA Technical Note D-7818*, 1974.
- [23] T.S. Beddoes, "A Synthesis of Unsteady Aerodynamic Effects including Stall Hysteresis", *Vertica*, Volume 1, No. 2, 1976.
- [24] T. Theodorsen and I.E. Garrick, "Non-Stationary Flow About a Wing-Aileron-Tab Combination Including Aerodynamic Balance", *NACA Technical Report 736*, 1942.
- [25] J.G. Leishman, "Unsteady Lift of a Flapped Airfoil by Indicial Concepts", *Journal of Aircraft*, Volume 31, No. 2, 1994.
- [26] N. Hariharan and J.G. Leishman, "Unsteady Aerodynamics of a Flapped Airfoil in Subsonic Flow by Indicial Concepts", *Journal of Aircraft*, Volume 33, No. 5, 1996.
- [27] C. Houbolt and G.W. Brooks, "Differential Equations of Motion for Combined Flapwise

- Bending, Chordwise Bending, and Torsion of Twisted Nonuniform Rotor Blades”,
NACA Report 1346, 1957.
- [28] W. Johnson, “Self-Tuning Regulators for Multicyclic Control of Helicopter Vibration”,
NASA Technical Paper 1996, 1982.
- [29] R. Cribbs and P.P. Friedmann, “Actuator Saturation and its Influence on Vibration Re-
duction by Actively Controlled Flaps”, Proceedings of the 42nd
AIAA/ASME/ASCE/AHS/ASC Structures, Structural Dynamics and Material Confer-
ence, Seattle, WA, April 2001.